International Journal of Automotive Manufacturing and Materials

Scilight

Review

Future High-Efficiency and Zero-Emission Argon Power Cycle Engines: A Review

Chenxu Wang, Shaoye Jin, Jun Deng, Weiqi Ding, Yongjian Tang, and Liguang Li *

School of Automotive Studies, Tongji University, Shanghai 200092, China
* Correspondence: liguang@tongji.edu.cn

Received: 27 February 2023
Accepted: 23 May 2023
Published: 13 Jun 2023

Abstract: This paper reviews the theoretical and experimental researches on Argon Power Cycle (APC) engines. Hydrogen-fueled APC is an innovative power system for a high efficiency and zero emissions, which employs argon rather than nitrogen as a diluent. Due to the large specific heat ratio of argon, the thermodynamic efficiency of APC engines is significantly higher compared to conventional internal combustion engines. However, APC engines face the challenge of knock inhibition, especially when using hydrogen as a fuel. Therefore, this paper summarizes the strategies and technologies to suppress the knock of hydrogen-fueled APC engines, including using alternative fuels with greater anti-knock capacity, lean combustion, and water injection. Furthermore, some guidance opinions are also provided for reference about the development and industrialization of APC engines, such as ultra-lean combustion, which uses pistons with thermal insulation coatings, employing low-friction lubricants, and developing efficient multi-component membrane separation system for argon separation.

Keywords: Argon Power Cycle (APC); hydrogen; high efficiency; knock inhibition; zero emission

1. Introduction

The target of peak carbon emissions and carbon neutrality has become the primary direction for the transportation and power industries in many countries. To achieve this target, China's internal combustion engine (ICE) industry has accordingly proposed the goals of the high efficiency, the low carbon, and near zero emissions. Meanwhile, the development of innovative power systems and the application of carbon-neutral fuels are recommended [1].

Argon Power Cycle (APC) is a novel power system for a higher efficiency and zero emissions [2]. In APC, the working substance is the argon (Ar), the oxide is oxygen, and the fuel is not limited. Ar is selected because it is the third rich gas, being of 0.93% in the atmosphere, much richer compared with other noble gases [3]. Figure 1 illustrates the principle of APC with hydrogen as the fuel. The higher specific heat ratio of Ar (1.67) than N_2 (1.40) is the critical factor in achieving high efficiency. When hydrogen is employed as fuel, the theoretical combustion products of APC engine are only the argon and the water, with zero NO_x and zero carbon emissions [4].

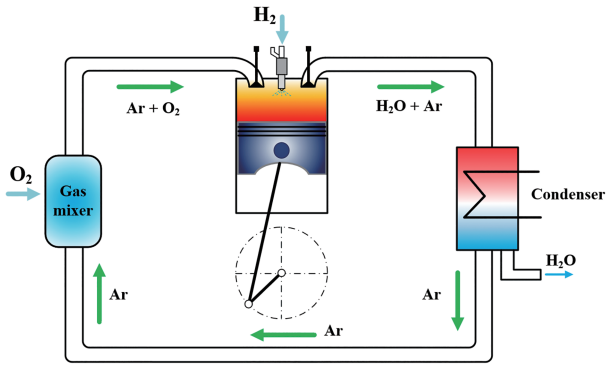

Figure 1. The principle of Argon Power Cycle (APC) with hydrogen as the fuel.

In previous studies, the APC engine has experimentally realized an indicated thermal efficiency of close to 50% by spark ignition (SI) [5] and compression ignition (CI) [6] with H_2 as the fuel. The researchers introduced APC into the ICE for different reasons [7–10]. De Boer et al. [5] employed Ar as a diluent to improve the combustion process of hydrogen-fueled ICEs and found that Ar provided significant efficiency improvements when the Ar molar ratio (AR) in the Ar-O_2 mixture was above 75%. Ikegami et al. [6] used Ar to achieve a higher in-cylinder temperature for the CI of H_2. Later researchers pointed out that the increase in efficiency was mainly caused by the high specific heat ratio of Ar, which can be predicted by thermodynamic theories [11–13].

Despite the great potential of high efficiency and zero emissions, the SI H_2-fueled APC engine faces the challenge of knocking [14]. Due to the higher in-cylinder temperature and pressure, the knock of the hydrogen-fueled APC engine is more serious than the normal hydrogen-fueled engine. To suppress the knock, some approaches and technologies have been studied, including increasing the AR [15], lean combustion [16], using the alternative fuels CH_4 [17, 18] and isooctane, lowering the intake temperature [19, 20], and water injection [21]. Prior to the hydrogen era, low carbon fuels, such as CH_4, are also available for APC engines. However, an effective carbon capture and recovery device is necessary for zero-emissions.

Another challenge of APC is the closed cycle of Ar. Unlike the air, the Ar cannot be supplied unlimitedly. Therefore, the Ar should be effectively separated and recycled. Kuroki et al. [11] designed and tested a closed cycling system for a hydrogen-fueled APC engine. Since the impurity is thought to be only steam, the cycling system consists mainly of a condenser. In Kuroki's study, this closed cycling system ran successfully for 40 min. However, the accumulation of CO_2 was also observed, which was blamed on the combustion of lubricant oil. Therefore, a CO_2 separator is needed in an argon closed-cycle system. An efficient multi-component membrane separation system may be a feasible solution for argon separation [22, 23].

Even so, the APC has its unique value and a great application prospect [24, 25]. Theoretically, ICE belongs to the heat engine, which is a machine to convert heat into work and can fundamentally be described by thermodynamic theories. For an Otto cycle, the compression ratio and the specific heat ratio are two determinate parameters for efficiency. APC technology is a feasible method to raise the specific heat ratio of the working substance to the physical limit. Therefore, the APC engine, together with the high compression ratio, is a promising concept for reaching the thermodynamic limit of ICE.

This paper presents a review of the APC-related researches, including theoretical and experimental studies. Firstly, a novel theoretical analysis method that can be widely applied to the performance prediction of various power cycle systems is presented in detail. Besides, the effects of crucial parameters on both efficiency improvement and knock suppression in APC engines are summarized. Finally, this paper provides guidance opinions for further research of APC engines.

2. Research Status

2.1. Theoretical Analysis

The theoretical analysis enables a great evaluation of engine performance boundaries, especially for new combustion concepts with novel thermodynamic cycles. It includes the thermodynamic and chemical kinetic analysis. The results of the theoretical analysis can provide a helpful reference for subsequent prototype design and experimental studies.

Engine in-cylinder temperature and pressure directly affect the efficiency and the anti-knock capability, which are affected by the diluent type. Therefore, the temperature and pressure at the end of compression and combustion are calculated with N_2, Ar, and CO_2 as diluents. The results show that the temperature and pressure are in the order of Ar, N_2, and CO_2 from high to low [13]. This phenomenon is because Ar has the highest specific heat ratio, while CO_2 has the lowest specific heat ratio. The study also indicated that decreasing the molar ratio of the fuel in the mixture can reduce the combustion temperature and pressure, thus increasing the compression ratio of the APC engine.

Efficiency is an important evaluation indicator for ICEs. In theoretical analysis, the efficiency calculation method should be applied to various power systems; namely, the method needs to be universal. Nevertheless, the real engine processes are complicated for theoretical calculation. Therefore, it is necessary to simplify the real engine processes and specify the different losses in each step of the energy transfer process. Decoupling efficiency allows for a better analysis of losses. Therefore, Professor Bengt Johansson [26] proposed Equation (1) to describe the relationships between various efficiencies of ICE:

$$\eta_{Brake} = \eta_{Combustion} \cdot \eta_{Thermodynamic} \cdot \eta_{GasExchange} \cdot \eta_{Mechanical} \tag{1}$$

where η_{Brake} refers to brake thermal efficiency, $\eta_{Combustion}$ refers to combustion efficiency, $\eta_{Thermodynamic}$ refers to thermodynamic efficiency, $\eta_{GasExchange}$ refers to gas exchange efficiency and $\eta_{Mechanical}$ refers to mechanical efficiency. In a conventional ICE, $\eta_{Combustion}$, $\eta_{GasExchange}$, and $\eta_{Mechanical}$ are usually higher than 90%, while $\eta_{Thermodynamic}$ is the lowest and has a limit of about 50–60%. Therefore, in the theoretical analysis, the focus should be on $\eta_{Thermodynamic}$. Meanwhile, to maintain the universality of the calculation results, the heat transfer loss and time loss in $\eta_{Thermodynamic}$ are not considered in the theoretical analysis. Equation (2) is a common and universal method for calculating $\eta_{Thermodynamic}$:

$$\eta_{Otto} = 1 - \frac{1}{\varepsilon^{\gamma - 1}} \tag{2}$$

where η_{Otto} is the Otto cycle efficiency, γ is the specific heat ratio, and ε is the compression ratio. Equation (2) clearly reveals the effects of γ and ε on η_{Otto}, but its calculation results are far from the real $\eta_{Thermodynamic}$ in engines. Thus, exploring a new calculation method to narrow the large gap between the theoretical and experimental values is significant.

In exploring the $\eta_{Thermodynamic}$ boundary of the hydrogen-fueled APC engine, Jin et al. [16] proposed an enhanced Otto cycle by combining the traditional Otto cycle with chemical equilibrium. Following this, Wang et al. [27] broadened it to the Miller cycle and named it the modified Miller cycle. Since the essences of these two models are the same, this paper refers to this model as the variable specific heat ratio Otto/Miller cycle (VKO/VKM). Figure 2 shows the calculation processes of VKO (1-2-3-4O-1) and VKM (1-2-3-4M-1M). In the VKO and VKM, Process 2–3 is a constant-volume adiabatic combustion process instead of a constant-volume heating process in the traditional Otto/Miller cycle. Other processes are reasonable simplifications of the engine cycle, so they have not been changed compared to the traditional Otto and Miller cycle. The State $4M_{max}$ is the limiting boundary of VKM.

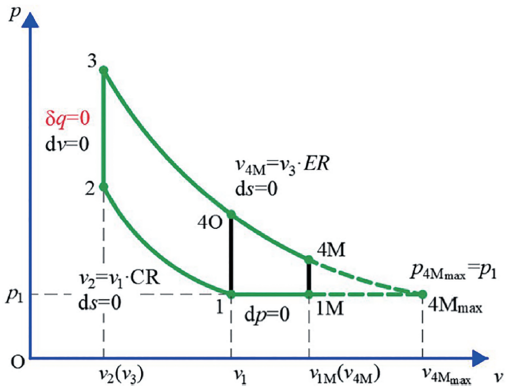

Figure 2. Diagram of the variable specific heat ratio Otto/Miller cycle. Reprinted with permission from [27].

Compared with the traditional Otto and Miller cycle, in the VKO and VKM, the effects of changing composition and a temperature-dependent specific heat ratio are considered. Thus, the thermodynamic efficiencies of VKO (η_{VKO}) and VKM (η_{VKM}) are lower than those of the traditional Otto/Miller cycle, but are still the upper limits of the efficiency of real engines. The η_{VKO} and η_{VKM} are calculated by Equations (3) and (4), respectively:

$$\eta_{VKO} = \frac{u_1 - u_{4O}}{\text{LHV}} \tag{3}$$

$$\eta_{VKM} = \frac{u_1 - u_{4M}}{\text{LHV}} \tag{4}$$

where u_1, u_{4O}, and u_{4M} are the specific internal energies at each state in Figure 2, and LHV is the lower heating value of the mixture composition at State 1.

In a specific condition, the experimental values of $\eta_{Thermodynamic}$ accounted for 65% and 70% of η_{Otto} and η_{VKO}, respectively [13,27]. As an upper limit of the efficiency prediction, a high proportion means a smaller gap and, therefore, more precise. Furthermore, chemical equilibrium is governed by the second law of thermodynamics. Thus, the calculation results of VKO and VKM still keep the universality of the thermodynamic calculation.

Figure 3 demonstrates the η_{VKM} boundaries of hydrogen-fueled APC engines with AR from 71% to 99% and compression ratio between 5–19. The η_{mi} in Figure 3 is the η_{VKM} in this paper. At a specific condition of compression ratio = 7 and AR = 91%, the η_{VKM} of hydrogen-fueled APC engine reaches 70%. In comparison, at the same compression ratio of 7, the η_{VKM} of a conventional hydrogen-fueled engine with air is only 52%, reducing by about 26% than APC engines [27].

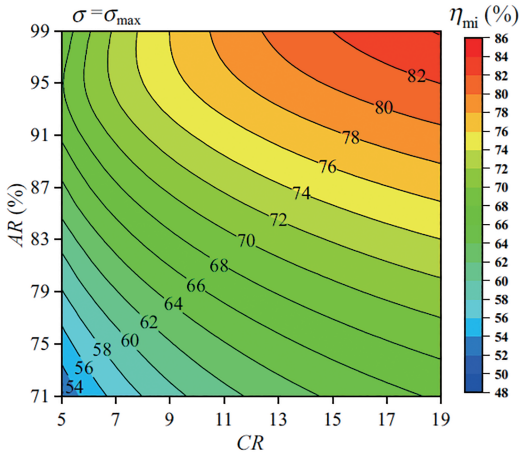

Figure 3. Thermodynamic efficiency boundaries of hydrogen-fueled APC engines. Reprinted with permission from [27].

To visualize the effects of main parameters or technologies on the performance of the hydrogen-fueled APC engine, an innovative four-quadrant diagram was presented [16] as Figure 4. In this figure, a specific reference point of compression ratio = 9 is first established. Each line presents one changed parameter. Studied parameters include the molar ratio of argon ratio in the mixture, replacing H_2 with CH_4 or NH_3, excess oxygen ratio (λ), and the molar ratio of H_2O in the Ar-O_2-H_2O mixture. The vertical axis indicates the difference in thermodynamic efficiencies between each point and the reference point. And $\tau-\tau_{ref}$ in the horizontal axis represents the ratio of the ignition delay time (an evaluation indicator of anti-knock property). The results indicated that increasing argon ratio and λ can simultaneously increase the efficiency and ignition delay time. The alternative fuels CH_4 and NH_3 have a greater anti-knock capacity than H_2. Nevertheless, if CH_4 and NH_3 are used as fuels, C and N will be introduced into the combustion products of APC, which makes argon separation more difficult. Adding water can raise the ignition delay time, thus may suppress the knock. However, it also leads to a significant reduction in efficiency. For example, with a compression ratio of 9.0 and an argon ratio of 95%, when the molar ratio of H_2O increases from 0 to 20%, the efficiency decreases from 70.2% to 64.4%. To balance the efficiency and power density of the hydrogen-fueled APC engine, a similar four-quadrant diagram method was also used by Wang et al. [27] and the results indicated that the optimal range of the ratio between the expansion ratio and the compression ratio was 1.5–2.0.

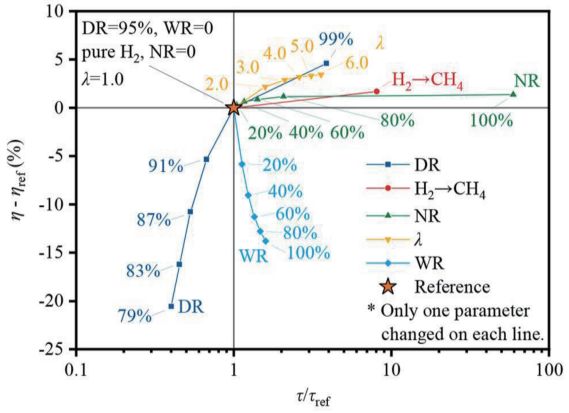

Figure 4. A comprehensive evaluation of the efficiency improvement and anti-knock capability of some potential methods. Reprinted with permission from [16]. (DR: dilution ratio, namely AR in this paper; NR: the molar ratio of NH_3 in the NH_3-H_2 mixture; WR: the molar ratio of H_2O in the Ar-O_2 mixture).

2.2. Efficiencies

Table 1 summarizes the publicly available information on typical APC prototypes. In Table 1, the highest indicated thermal efficiencies of H_2-fueled and CH_4-fueled APC engines were obtained by Manuel Cech et al. [28] and Jin et al. [29], respectively. The highest indicated thermal efficiency of 55% is achieved at compression ratio of 15.5 with direct hydrogen injection. According to Figure 3, the thermodynamic efficiency boundary of hydrogen-fueled APC is roughly 70–80% in the range of operating conditions of the real APC engine. Therefore, the indicated thermal efficiency of hydrogen-fueled APC engines still has a great potential for improvement.

Table 1. Summary of typical Argon Power Cycle (APC)'s prototypes.

First Address		Cornell University	Kyoto University	Toyota Motor Corporation	Lawrence Livermore National Laboratory	Tongji University			King Abdullah University of Science & Technology		University of California–Berkeley	WTZ GmbH
Year		1980	1982	2010	2011	2017	2021	2023	2019	2020	2021	2021
First author		De Boer [5]	Ikegami [6]	Kuroki [11]	Killingsworth [12]	Deng [15]	Jin [29]	Jin [21]	Mohammed [31]	Elkhazraji [19]	Shi [17]	Manuel Cech [28]
Displacement (L)		-	0.815	0.500	0.616	0.808	1.0	1.0	0.612	0.612	0.611	-
Cylinder number		1	1	1	1	1	3	3	1	1	1	1
Bore (mm)		-	95	86	82.5	95	73.4	73.4	82.55	82.55	82.5	128
Stroke length (mm)		-	115	86	114	114	78.6	78.6	114.3	114.3	114.3	-
Compression ratio		5.5–12	12.3 (11.9) 16.0 (15.5)	6.0 (4.0)	4.5–7.0	10.5	12.5	9.6	8.8	13.2–15.2	8, 12.5	15.5
Speed (r/min)		460–1670	1200	1100	900	1200	1000	1000	600	600	600	-
Argon ratio (%)	$Ar/(Ar+O_2)$	-	79	88	-	-	79, 85, 90	80	79		79, 85, 90, 92.5	79
	$Ar/(Ar+O_2+fuel)$	50–90	-	-	84, 86, 88	75, 79, 82	-	-	-		-	-
Fuel		H_2	H_2	H_2	H_2	CH_4	CH_4	H_2	Isooctane	CH_4	CH_4	H_2
Fuel injection		premixed	DI	DI	PFI	PFI	PFI	PFI	PFI	PFI	PFI	DI
λ		1.0	-	0.88–1.92	1.0	1.0	1.00–2.15	1.0–5.67	2.5	4, 5	1.00–3.33	3.0
Ignition mode		SI	CI	SI	SI	SI	SI	SI	HCCI	HCCI	SI, HCCI, SACI	CI
IMEP (MPa)		0.34–0.65	0.18–0.94	0.32	-	-	0.3–1.19	0.25–0.61	0.38	0.20–0.28	0.12–0.88	0.55
Maximum Indicated thermal efficiency (%)		49	49	41	44.1	47.8	51.7	50.3	42	48.3	43.0	55

Studies have shown that the highest indicated thermal efficiency of hydrogen engines in air is often obtained at a speed close to 5000 r/min, and the highest brake thermal efficiency tends to be achieved at 2000–3000 r/min, as a result of the competition between heat transfer losses and mechanical losses [30]. Thus, in the subsequent research, it is necessary to increase the speed of APC engines and explore the optimal speed range.

Based on Equation (1), the η_{Brake} can be decoupled. Kuroki et al. [11] found that when λ was greater than 1.2, the $\eta_{Combustion}$ of APC engines could be close to 100%. Killingsworth et al. [12] indicated that the heat transfer loss at the same compression ratio is greater in the argon-oxygen atmosphere than in air. Through theoretical studies, Liu et al. [32] also demonstrated that the heat transfer losses rise with the promotion of the compression ratio. Ikegami et al. [6] pointed out that the mechanical losses of APC engines are larger than conventional engines due to the higher in-cylinder pressure. As shown in Figure 5a, with a compression ratio of 16 and a BMEP (Brake mean effective pressure) of 0.4 MPa, peak pressures in argon-oxygen mixture and air are 8.2 MPa and 6.8 MPa, respectively. At the same compression ratio and BMEP, by replacing the air with argon-oxygen mixture, the indicated thermal efficiency increases by 22%, while the brake thermal efficiency grows by less than 4%. The high mechanical losses in the argon-oxygen mixture results in a lower gain in brake thermal efficiency than the indicated thermal efficiency.

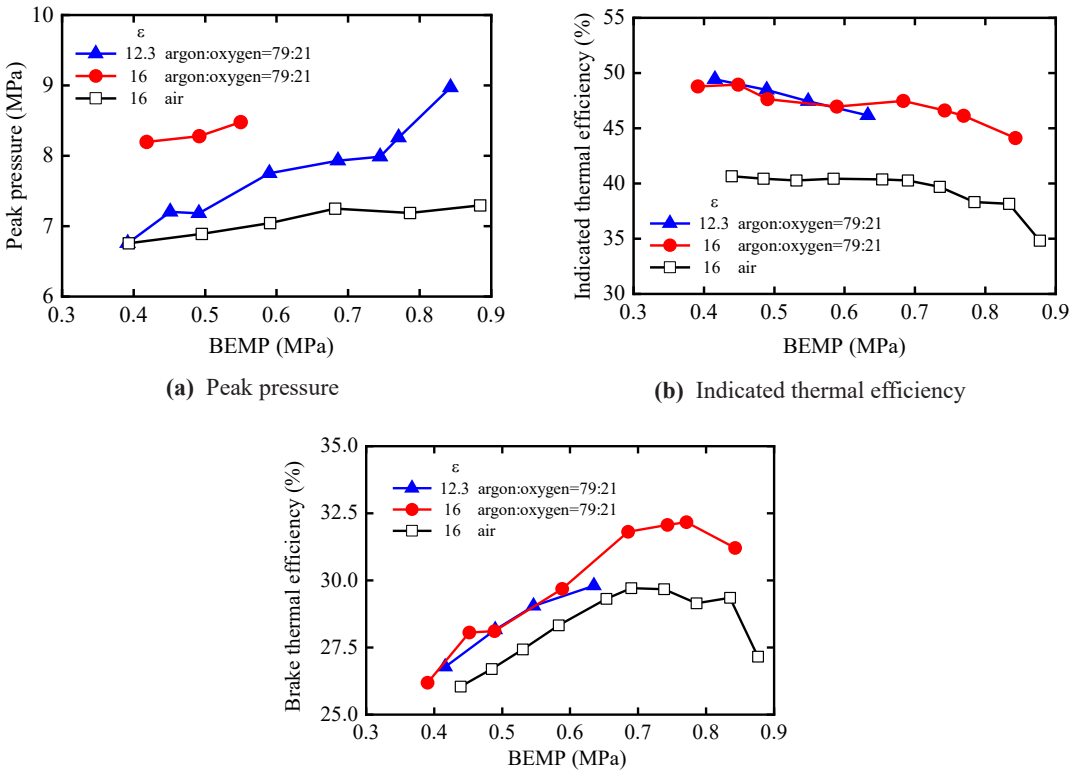

(a) Peak pressure

(b) Indicated thermal efficiency

(c) Brake thermal efficiency

Figure 5. Main performances of a CI hydrogen engine in argon-oxygen mixture and air. Reprinted with permission from [6].

For the APC engine, the $\eta_{Combustion}$ and $\eta_{GasExchange}$ are easily close to 100%. The larger heat transfer loss and the lower $\eta_{Mechanical}$ limit the improvement of the indicated thermal efficiency and the brake thermal efficiency, respectively. Because of the high in-cylinder temperature and pressure, the heat transfer efficiency (the ratio between the indicated thermal efficiency and $\eta_{Thermodynamic}$) is usually less than 80%, and the mechanical efficiency is much lower than 90% [13]. Increasing the engine speed may reduce the heat transfer loss while leading to an increase in mechanical loss. Using pistons with thermal insulation coating materials [33–35] and employing low-friction lubricants [36–38] may be feasible ways to reduce these losses.

2.3. Knock and Compression Ratio

The APC engine takes advantage of the high specific heat ratio of argon to improve efficiency. However, the high specific heat ratio also raises the in-cylinder temperature and pressure, thus promoting the knock [39]. In Table 1, due to the limitation of knock, the compression ratios of SI hydrogen-fueled APC engines are generally lower than 10. De Boer et al. [5] tested the compression ratios of 5.5 to 12 and obtained the highest indicated thermal efficiency at 7. Killingsworth et al. [12] studied a range of compression ratios from 4.5 to 7 and achieved a maximum indicated thermal efficiency of 44.1% at 5.5. By water direct injection in the late exhaust stroke to inhibit the knock, Jin et al. [21] achieved the normal operation at a compression ratio of 9.6. Based on the published data, the compression ratio of 9.6 is the highest in the SI hydrogen-fueled APC engine without knocking.

Killingsworth et al. [12] analyzed the effects of increasing compression ratio on the indicated thermal efficiency and the cyclic variation of indicated mean effective pressure (IMEP) in different atmospheres. In Figure 6, under the argon-oxygen atmosphere, the indicated thermal efficiency increases with the growths of compression ratio from 4.5 to 5.5; as the compression ratio continues to rise to 6.5, the indicated thermal efficiency remains stable; however, when the compression ratio is elevated to 7, the indicated thermal efficiency decreases sharply, and the engine cannot maintain the normal operation due to knocking. In contrast, under the air atmosphere, even if the compression ratio increases to 17, the engine can still run normally, and the indicated thermal efficiency is relatively insensitive to the change in compression ratio.

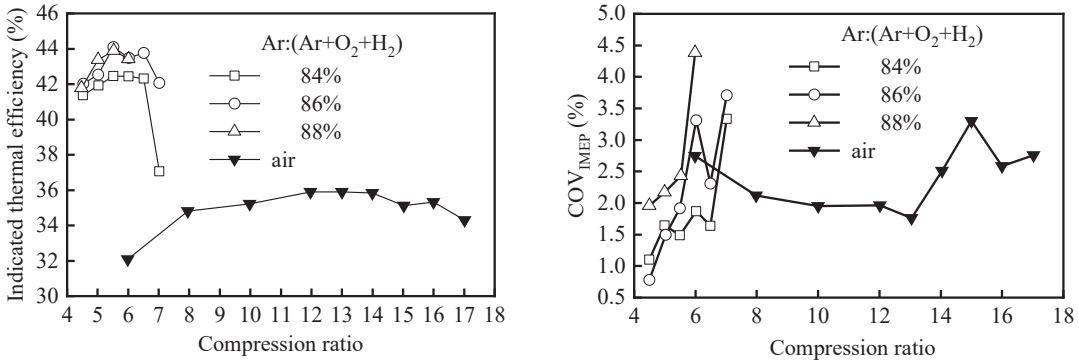

(a) Indicated thermal efficiency

(b) Cyclic variation of indicated mean effective pressure (IMEP)

Figure 6. Effects of compression ratio on the indicated thermal efficiency and cyclic variation in air and argon-oxygen atmosphere. Reprinted with permission from [12].

Knocking can promote the cyclic variation of APC engines. As shown in Figure 6, when the compression ratio is lower than 6, the cyclic variation of indicated mean effective pressure (COV_{IMEP}) is smaller in argon-oxygen atmosphere than in air. However, as the compression ratio increases, the COV_{IMEP} under argon-oxygen atmosphere continues to increase and will exceed that of air atmosphere. Figure 6 also shows that the COV_{IMEP} under air atmosphere can remain stable over a wide range of compression ratios. In contrast, under the argon-oxygen atmosphere, the COV_{IMEP} is more sensitive to the change in compression ratio. In both atmospheres, the cyclic variation is below the stability threshold of 5% and could be less than 2% in some conditions.

In addition, the knock can also delay the combustion phase. Figure 7 demonstrates that with a compression ratio of 7, the CA50 exceeds 40 and 30°CA ATDC at argon ratio of 84% and 86%, respectively. Even when the compression ratio is reduced to 4.5, the CA50 generally exceeds 10° CA ATDC at all operating conditions. Heywood et al. [40] concluded that the CA50 at the highest efficiency point ranged from 5 to 7° CA ATDC. Manuel Cech et al. [28] indicated that the optimal CA50 range in terms of efficiency is 4.5–6°CA ATDC and 6–8°CA ATDC in Ar-O_2 and air atmosphere, respectively. Therefore, the serve knock of the hydrogen-fueled APC engine may overly delay the ignition time and prevent the full efficiency potential of APC [12].

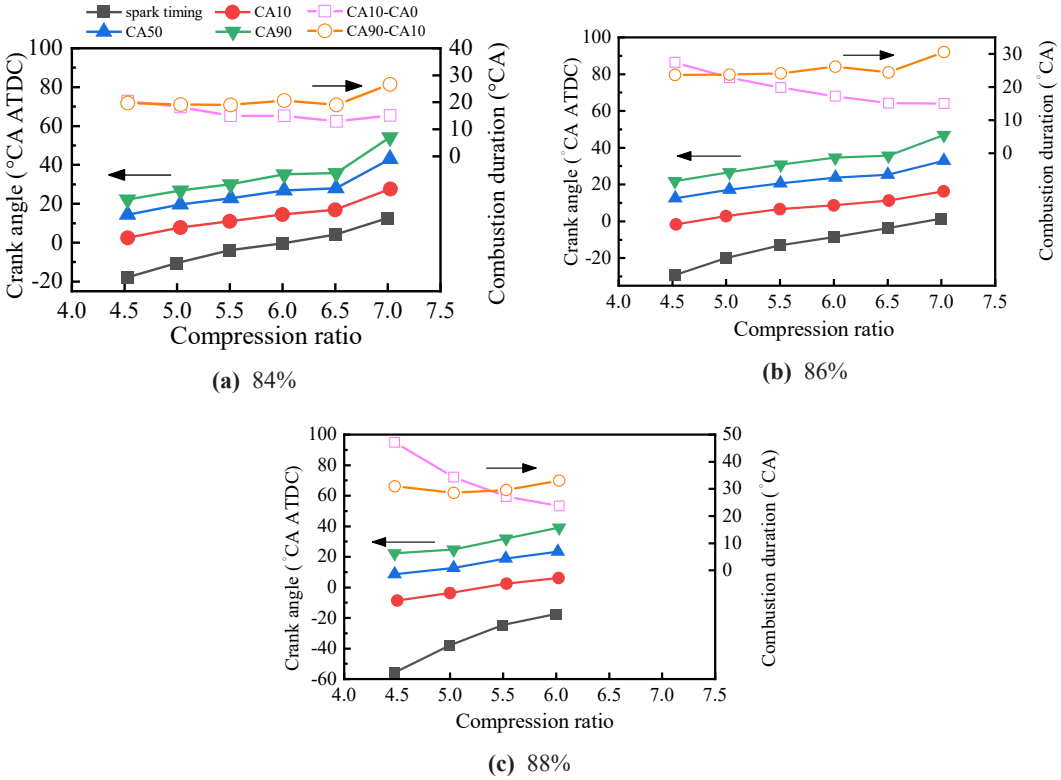

Figure 7. Effects of compression ratio on the combustion phase of APC engines with the different argon ratios in argon-oxygen-hydrogen mixture. Reprinted with permission from [12].

2.4. Knock Inhibition Strategies

2.4.1. Using Alternative Fuels

H_2 is generally considered to have a great anti-knock capacity in air environment of combustion engines, with a Research Octane Number (RON) of 120 to 140 [40]. Studies by Ford have shown that the compression ratio of hydrogen engines can reach 15.3 even in the mode of port injection [30].

However, the anti-knock capacity of a fuel is related to the test method or standard. Depending on different test methods, Verhelst et al. [41] concluded that the RON of H_2 may be distributed in the range of 88 to 130. Moreover, if the standard of Motor Octane Number (MON) is used, the MON of H_2 may be lower than 60. RON and MON are not the only criteria for anti-knock capacity. For example, with the mass application of natural gas, it has been found that the RON and MON traditionally applied to the gasoline are not applicable to gaseous fuels. Thus, the concept of Methane Number (MN) is introduced. In the MN criterion, CH_4 and H_2 are chosen as the reference fuels, with the CH_4 set to 100 MN due to its high anti-knock capacity and the H_2 set to 0 MN due to its low anti-knock capacity.

Therefore, the replacement of H_2 by natural gas is expected as a potential approach to suppress knock and thus improve the efficiency of APC engines. In a port injection CFR engine, De Boer et al. [5] and Killingsworth et al. [12] obtained the highest indicated thermal efficiency with H_2 as fuel and spark ignition at compression ratios of 7 and 5.5, respectively. By replacing H_2 with natural gas, Shi et al. [17] achieved a higher compression ratio of 12.5 in all three modes: spark ignition, homogeneous charge compression ignition (HCCI), and spark-assisted compression ignition (SACI). In these three modes, the highest indicated thermal efficiency of 43% was obtained in SACI mode at λ = 2.0 and argon ratio of 85%. Meanwhile, the IMEP at the highest efficiency is 0.43 MPa.

In addition, Mohammed et al. [31] also studied the use of isooctane as an alternative fuel. The inlet pressure is set at 0.1 MPa, the speed is 600 r/min, and the HCCI mode is used. By adjusting the compression ratio, the CA50 is controlled at the compression top dead center (TDC). When the inlet gas composition is the argon-oxygen mixture with an argon ratio of 80%, the compression ratio could reach 8.8. As a comparison,

when the inlet gas composition is the air, or the mixture of N_2:O_2 is 80:20, the compression ratio could arrive at 15. Meanwhile, under the argon-oxygen and air atmosphere, the indicated thermal efficiencies are about 40% and 42%, respectively. This study indicates that the compression ratio range for APC engine operation can be expanded by employing isooctane as the fuel.

2.4.2. Lean Combustion

The essence of lean combustion is to reduce the proportion of fuel in the mixture. Lean combustion can reduce the combustion temperature and pressure, thus suppressing the knock and reducing the heat transfer loss.

The high specific heat ratio of argon facilitates a higher in-cylinder temperature and pressure, thus expanding the flammable range of the fuel. Therefore, in APC engines, the λ boundary is higher than that of conventional engines. Based on a CH_4-SI APC engine, Shi et al. [17] experimentally verified that argon has a broadening effect on the boundary of λ. The results indicated that at a compression ratio of 12.5, the λ boundary of CH_4 is expanded from 1.5 to 3.3 by replacing N_2 with argon [17]. With the increase of λ, the spark-ignition time and the combustion phase are advanced, and the peak pressure is closer to TDC. It means that the CA50 can be controlled in the optimal range by adjusting λ. In a CH_4-CI APC engine, Aznar et al. [42, 43] also found that increasing λ can optimize the CA50 and time loss, thereby improving the efficiency.

H_2 has a wider flammable range than CH_4 [44], leading to a greater range in λ. In a PI-SI-APC hydrogen engine, the highest indicated thermal efficiency of 50.32% is obtained at λ of 2.6 [21]. Nevertheless, when using CH_4 as the fuel, although with a higher CR of 12.5, the boundary of λ is 2.11 [29]. A theoretical study also indicated that when the λ is larger than 3, the effect of increasing λ on knock suppression and efficiency improvement is not significant [16]. Therefore, to find the optimal range of λ, further experimental studies should be performed on the APC engine.

Moreover, for the APC engine, the growth of argon ratio can also reduce the fuel percentage in the mixture. Therefore, increasing argon ratio is also a potential approach to suppress knocking and improve efficiency.

2.4.3. Water Injection

Water injection can inhibit knocking through its dilution and cooling effects [45, 46]. Usually, water injection is divided into a port injection or in-cylinder direct injection. According to Figure 4, premixing water with the initial mixture can increase the ignition delay time and suppress the knock. However, it also reduces the thermodynamic efficiency. For a four-stroke engine, the cycle work is mainly determined by the compression and expansion processes. Therefore, to reduce the negative impact of water injection on the efficiency, Jin et al. [21] proposed directly injecting water into the cylinder during the late exhaust stroke. By this measure, the compression ratio of the H_2-SI APC engine is broadened from 6.5 (the maximum compression ratio of engine operation in Killingsworth's study [12]) to 9.6, and the highest indicated thermal efficiency of 50.32% is achieved. Meanwhile, the study also found that delaying the water injection time has a slight effect on the combustion phase and combustion duration.

2.4.4. Sub-zero Intake Temperature

The lower intake temperature reduces the in-cylinder temperature and pressure, thereby suppressing knocking and promoting compression ratio. Based on a CFR engine, Elkhazraji et al. [19] studied the anti-knock effect of lowing intake temperatures in an HCCI CH_4-fueled APC engine. The results indicated that the sub-zero intake temperature enables the engine to run at a higher compression ratio. For example, at λ of 4, when the intake temperature reduces from 40 °C to −6 °C, the compression ratio can be elevated from 13.2 to 15.1. However, the cooled charge causes more pumping losses, thus reducing the $\eta_{GasExchange}$. Meanwhile, the reduced in-cylinder temperature deteriorates the combustion process, which leads to a decrease in $\eta_{Combustion}$. Thus, despite the reduced heat transfer losses, the indicated thermal efficiency decreased by 7%.

3. Conclusions and Perspectives

This paper presents a review on future high-efficiency and zero-emission APC engines. Researches on

the efficiency improvement and the knock inhibition are summarized. In addition, a novel thermodynamic analysis method suitable for exploring the performance boundaries of power systems is recommended. The main conclusions and perspectives are as follows:

(1) APC engines offer a high potential for efficiency improvement compared to conventional engines. Due to the high specific heat ratio of argon, APC engines can reach thermodynamic efficiency of 70–80%, while that of conventional gasoline or diesel engines is between 50% and 60%.
(2) Knocking limits the increase of compression ratio and efficiency in APC engines, especially when H_2 is used as the fuel. The use of alternative fuels with a greater anti-knock capacity (such as CH_4), lean combustion, and water injection have been shown to be viable approaches for knocking suppression in APC engines.
(3) Because of the higher in-cylinder temperature and pressure generated by the argon, methods to reduce the heat transfer loss and mechanical loss should also be considered. Increasing the rotational speed to 2000–3000 r/min, implementing ultra-lean combustion ($\lambda > 4$), using pistons with thermal insulation coatings, and employing low-friction lubricants are worth trying.
(4) The realization of a closed cycle of argon is a prerequisite for the industrialization of APC engines. Nevertheless, even with hydrogen-fueled APC engines, the accumulation of CO_2 is still observed in the exhaust due to the combustion of lubricant oil. Therefore, to achieve the zero emissions, it is necessary to develop efficient argon separation and carbon capture systems suitable for vehicles, especially when using carbon-based fuels (such as CH_4). A multi-component membrane separation system may be a feasible solution.
(5) The large amount of water produced by H_2 combustion significantly promotes lubricant emulsification. The effects of water on lubricant emulsification should be further studied and a special lubricant should be applied in the APC engines.

Author Contributions: Conceptualization and methodology, L.L., J.D., C.W., S.J.; literature review and resources, C.W., S.J.; writing, C.W.; editing, L.L., J.D., W.D., and Y.T.; funding acquisition, L.L. and J.D. All authors have read and agree to the published version of the article.

Funding: This research was funded by the National Natural Science Foundation of China [grant numbers 52076153 and T2241003] and the Shanghai Science and Technology Program [grant number 22ZR1463000].

Data Availability: Statement: Not applicable.

Conflicts of Interest: The authors declare no conflict of interest.

References

1. Wang, L.; Hong, C.; Li, X.; et al. Review on blended hydrogen-fuel internal combustion engines: A case study for China. *Energy Reports* **2022**, *8*, 6480–6498. doi: 10.1016/j.egyr.2022.04.079.
2. Li, L.; Gong, Y.; Deng, J.; et al. CO2 Reduction Request and Future High-Efficiency Zero-Emission Argon Power Cycle Engine. *Automotive Innovation* **2018**, *1*(1), 43–53. doi: 10.1007/s42154-018-0007-y.(In Chinese)
3. Park S. Y.; Kim J. S.; Lee J. B.; et al. A redetermination of the argon content of air for buoyancy corrections in mass standard comparisons. *Metrologia* **2004**, *41*(6), 387–395. doi: 10.1088/0026-1394/41/6/005.
4. Dibble, R. The Iron "Fuel Cell" Argon Engine Project. *Changchun Auto Mobile Show, China*, **2013**.
5. de Boer, P. C. T.; Hulet J. F. Performance of a Hydrogen-Oxygen-Noble Gas Engine. *International Journal of Hydrogen Energy* **1980**, *5*(4), 439–452. doi: 10.1016/0360-3199(80)90024-5.
6. Ikegami, M.; Kei, M.; and Masahiro S. A study of hydrogen fuelled compression ignition engines. *International Journal of Hydrogen Energy* **1982**, *7*(4), 341–353. doi: 10.1016/0360-3199(82)90127-6.
7. Prashanth, K.; Shaik A. Experimental investigation of argon gas induction on diesel engine performance and emission characteristics: A comprehensive study on de-NOx techniques. *Process Safety and Environmental Protection* **2021**, *152*, 471–481. doi: 10.1016/j.psep.2021.06.036.
8. Taib, N. M.; Mansor, M. R. A.; Mahmood W. M. F. W. Combustion characteristics of hydrogen in a noble gas compression ignition engine. *Energy Reports* **2021**, *7*, 200–218. doi: 10.1016/j.egyr.2021.07.133.
9. Morovatiyan, M.; Shahsavan, M.; Aguilar, J.; et al. Effect of Argon Concentration on Laminar Burning Velocity and Flame Speed of Hydrogen Mixtures in a Constant Volume Combustion Chamber. *Journal of Energy Resources Technology, Transactions of the ASME* **2021**, *143*, 3. doi: 10.1115/1.4048019.
10. Taib, N.M.; Mansor, M.R.A.; Mahmood W.M.F.W. Combustion characteristics of direct injection hydrogen in noble gases atmosphere. In *IOP Conference Series: Earth and Environmental Science*. IOP Publishing: Bristol, UK, 2020, *463*, no. 1. doi: 10.1088/1755-1315/463/1/012058.
11. Kuroki, R.; Kato, A.; Kamiyama, E.; et al. Study of high efficiency zero-emission argon circulated hydrogen engine. *SAE Technical Papers* **2010**, 2010-01-0581. doi: 10.4271/2010-01-0581.

12. Killingsworth, N.J.; Rapp, V.H.; Flowers, D.L.; et al. Increased efficiency in SI engine with air replaced by oxygen in argon mixture. *Proceedings of the Combustion Institute* **2011**, *33*(2), 3141–3149. doi: 10.1016/j.proci.2010.07.035.
13. Jin, S.; Deng, J.; Gong, X.; et al. Thermodynamic Analysis on Factors Influencing the Thermal Conversion Efficiency of the Argon Power Cycle Engine. *Transactions of CSICE* **2020**, *38*(04), 351–358. doi: 10.16236/j.cnki.nrjxb.202004046.
14. Killingsworth, N.; Rapp, V.; Flowers, D.; et al. *Characteristics of knock in hydrogen-oxygen-argon SI engine* (No. *LLNL-CONF-424554).* Western States Section of the Combustion Institute Spring Technical Meeting 2010, no. December 2015, pp. 772–778, 2010.
15. Deng, J.; Gong, X.; Zhan, Y.; et al. Experiment on combustion characteristics of natural gas in cylinder under Ar-O2 atmosphere. *Transactions of CSICE* **2017**, *35*(1), 38–43, doi: 10.16236/j.cnki.nrjxb. 201701006.
16. Jin, S.; Deng, J.; Li L. Thermodynamic and Chemical Analysis of the Effect of Working Substances on the Argon Power Cycle. *SAE Technical Papers* **2021**, 2021-01-0447.
17. Shi, S.; Tomomatsu, Y.; Chaturvedi, B.; et al. Engine efficiency enhancement and operation range extension by argon power cycle using natural gas. *Applied Energy* **2021**, *281*, 116109, doi: 10.1016/j.apenergy.2020.116109.
18. Drost, S.; Aznar M. S.; Schießl, R.; et al. Reduced reaction mechanism for natural gas combustion in novel power cycles. *Combust Flame* **2021**, *223*, 486–494. doi: 10.1016/j.combustflame.2020.09.029.
19. Elkhazraji, A.; Mohammed, A.; Jan, S.M.; et al. On Maximizing Argon Engines' Performance via Subzero Intake Temperatures in HCCI Mode at High Compression Ratios. *SAE Technical Papers* **2020**, 2020-01-1133.
20. Jan, S.M.; Mohammed, A.; Elkhazraji, A.; et al. The Road Towards High Efficiency Argon SI Combustion in a CFR Engine: Cooling the Intake to Sub-Zero Temperatures. *SAE Technical Papers* **2020**, 2020-01-0550.
21. Jin, S.; Deng, J.; Wang, C.; et al. Knock Inhibition in Hydrogen Fueled Argon Power Cycle Engine with a Higher Compression Ratio by Water Direct Injection at Late Exhaust Stroke. *SAE Technical Papers* **2023**, 2023-01-0227.
22. Sierra Aznar, M.; Chorou, F.; Chen, J.Y.; et al. Experimental and numerical investigation of the argon power cycle. Proceedings of the ASME 2018 Internal Combustion Engine Division Fall Technical Conference. Volume 1: Large Bore Engines; Fuels; Advanced Combustion. San Diego, California, USA. November 4–7, 2018. V001T01A006. ASME. doi: 10.1115/ICEF2018-9670.
23. Chourou, F.; Aznar, M.S.; Chen, J.Y.; et al. A new efficient model for multicomponent membrane separation and application to the Argon Power Cycle. In *2017 Fall Technical Meeting of the Western States Section of the Combustion Institute*, *WSSCI 2017*, no. October, 2017.
24. Hafiz, N.M.; Mansor, M.R.A.; Mahmood, W.M.F.W.; et al. Simulation of the Effect of Initial Temperature and Fuel Injection Pressure on Hydrogen Combustion Characteristics in Argon-Oxygen Compression Ignition Engine. *SAE Technical Papers* **2016**, 2016-01-2227. doi: 10.4271/2016-01-2227.
25. Hafiz, N. M.; Mansor, M. R. A.; Mahmood, W. M. F. W.; et al. Numerical study of hydrogen fuel combustion in compression ignition engine under argon-oxygen atmosphere. *Jurnal Teknologi* **2016**, *78*(6–10), 77–83. doi: 10.11113/jt.v78.9192.
26. Olsson, J. O.; Tunestål, P.; Ulfvik, J.; et al. The Effect of Cooled EGR on Emissions and Performance of a Turbocharged HCCI Engine. *SAE Technical Papers* **2003**, 2003-01-0743.
27. Wang, C.; Jin, S.; Deng, J.; et al. An Innovative Argon/Miller Power Cycle for Internal Combustion Engine: Thermodynamic Analysis of its Efficiency and Power Density. *Automotive Innovation* **2023**, *Jan*, 1–13. doi: 10.1007/s42154-022-00208-x.
28. Cech, M.; Knape, M.; Wilfert, T.; et al. The emission-free hydrogen closed-cycle engine. *MTZ worldwide* **2021**, *82* (04), 42–46.
29. Jin, S. Deng, J.; Liang, X. et al. Experimental Study on the Efficiency, Load, and Emissions of Methane-Fueled Argon Power Cycle Engine. Proceedings of China SAE Congress. *SAECCE*, **2021**. (In Chinese)
30. Tang, X.; Kabat, D. M.; Natkin, R. J.; et al. Ford P2000 Hydrogen Engine Dynamometer Development. *SAE Transactions* **2002**, 2002-01-0242.
31. Mohammed, A.; Masurier, J.; Elkhazraji, A.; et al. A path towards high efficiency using argon in an HCCI engine. *SAE Technical Papers* **2019**, 2019-01-0951. doi: 10.4271/2019-01-0951.
32. Liu, H.; Ma, J.; Tong, L.; et al. Investigation on the potential of high efficiency for internal combustion engines. *Energies (Basel)* **2018**, *11*(3), 513. doi: 10.3390/en11030513.
33. Y. Wakisaka *et al*.. Reduction of Heat Loss and Improvement of Thermal Efficiency by Application of "Temperature Swing" Insulation to Direct-Injection Diesel Engines. *SAE International Journal of Engines* **2016**, *9*(3), 1449–1459. doi: 10.2307/26284912.
34. Musthafa, M. M. Thermal barrier coated diesel engine running on biodiesel: a review. *International Journal of Sustainable Engineering* **2018**, *11*(3), 159–166. doi: 10.1080/19397038.2017.1393024.
35. Hazar, H.; Ozturk U. The effects of Al2O3-TiO2 coating in a diesel engine on performance and emission of corn oil methyl ester. *Renew Energy* **2010**, *35*(10), 2211–2216. doi: 10.1016/j.renene.2010.02.028.
36. Arai, K.; Yamada, M.; Asano, S.; et al. Lubricant Technology to Enhance the Durability of Low Friction Performance of Gasoline Engine Oils. *SAE Transactions* **1995**, *104*, 1964–1972. Available Online: http://www.jstor.org/stable/44615212
37. Vaitkunaite, G.; Espejo, C.; Thiebaut, B.; et al. Low friction tribofilm formation and distribution on an engine cylinder tested with MoDTC-containing low viscosity engine lubricants. *Tribology International* **2022**, *171*, 107551. doi: 10.1016/j.triboint.2022.107551.
38. Lee, P.; Zhmud B. Low friction powertrains: Current advances in lubricants and coatings. *Lubricants* **2021**, *9*(8), 74. doi: 10.3390/lubricants9080074.

39. Jin, S.; Huang, X.; Deng, J.; et al. Initiation characteristics of spark-ignited premixed hydrogen-oxygen flames with diluents of argon/nitrogen/carbon dioxide. *International Journal of Hydrogen Energy* **2021**, *46*(40), 21212–21221. doi: 10.1016/j.ijhydene.2021.03.234.
40. Heywood, J. B. *Internal Combustion Engine Fundamentals.* McGraw-Hill Education: New York City, NY, USA, 2018. *ISBN*:978-*1*-260-11610-6.
41. Verhelst, S.; Wallner T. Hydrogen-fueled internal combustion engines. *Progress in Energy and Combustion Science* **2009**, *35*(6), 490–527. doi: 10.1016/j.pecs.2009.08.001.
42. Sierra-Aznar, M.; Pineda, D. I.; Cage, B. S.; et al. Working fluid replacement in gaseous direct-injection internal combustion engines: A fundamental and applied experimental investigation. In *10th U. S. National Combustion Meeting*, Maryland, 2017.
43. Aznar, M. S.; Pineda, D. I.; Cage, B. S.; et al. Experimental Investigation of Port and Direct Injection Strategies for Internal Combustion Engines with Argon as the Working Fluid Combustion Research at LLNL View project Low Swirl Burner Down-Scaling View project. *Proceedings of the European Combustion Meeting* **2017**, 1–6. doi: 10.17605/OSF.IO/PT67Q.
44. Seboldt, D.; Mansbart, M.; Grabner, P.; et al. Hydrogen Engines for Future Passenger Cars and Light Commercial Vehicles. *MTZ worldwide* **2021**, *82*(2), 42–47. doi: 10.1007/s38313-020-0603-1.
45. Khatri, J.; Sharma, N.; Dahlander, P.; et al. Effect of relative humidity on water injection technique in downsized spark ignition engines. *International Journal of Engine Research* **2021**, *22*(7), 2119–2130. doi: 10.1177/1468087420940854.
46. Kang, Z.; Feng, S.; Lv, Y.; et al. Effect of direct water injection temperature on combustion process and thermal efficiency within compression ignition internal combustion Rankine engine. *Case Studies in Thermal Engineering* **2021**, *28*, 101592. doi: 10.1016/j.csite.2021.101592.

Citation: Wang, C X.; Jin, S Y.; Deng, J.; et al. Future High-Efficiency and Zero-Emission Argon Power Cycle Engines: A Review. *International Journal of Automotive Manufacturing and Materials* **2023**, *2*(2), 2.